HHS Public Access

Author manuscript

Biomaterials. Author manuscript; available in PMC 2018 May 01.

Published in final edited form as:

Biomaterials. 2017 May ; 127: 132–140. doi:10.1016/j.biomaterials.2017.02.010.

Elastin-like Protein-Hyaluronic acid (ELP-HA) Hydrogels with Decoupled Mechanical and Biochemical cues for Cartilage Regeneration

Danqing Zhu[*],
Department of Bioengineering, Stanford University, Stanford, CA 94305 (USA)

Huiyuan Wang[*],
Department of Materials Science & Engineering, Stanford University, Stanford, CA 94305, USA

Pavin Trinh,
Department of Bioengineering, Stanford University, Stanford, CA 94305 (USA)

Prof. Sarah C. Heilshorn[#], and
Department of Materials Science & Engineering, Stanford University, Stanford, CA 94305, USA;
Department of Materials Science & Engineering, Stanford University, Stanford, CA 94305 (USA)

Prof. Fan Yang[#]
Department of Bioengineering, Stanford University, Department of Orthopaedic Surgery, Stanford University, Stanford, CA 94305 (USA)

Abstract

Hyaluronic acid (HA) is a major component of cartilage extracellular matrix and is an attractive material for use as 3D injectable matrices for cartilage regeneration. While previous studies have shown the promise of HA-based hydrogels to support cell-based cartilage formation, varying HA concentration generally led to simultaneous changes in both biochemical cues and stiffness. How cells respond to the change of biochemical content of HA remains largely unknown. Here we report an adaptable elastin-like protein-hyaluronic acid (ELP-HA) hydrogel platform using dynamic covalent chemistry, which allows varyiation of HA concentration without affecting matrix stiffness. ELP-HA hydrogels were created through dynamic hydrazone bonds *via* the reaction between hydrazine-modified ELP (ELP-HYD) and aldehyde-modified HA (HA-ALD). By tuning the stoichiometric ratio of aldehyde groups to hydrazine groups while maintaining ELP-HYD concentration constant, hydrogels with variable HA concentration (1.5%, 3%, or 5%) (w/v) were fabricated with comparable stiffness. To evaluate the effects of HA concentration on cell-based cartilage regeneration, chondrocytes were encapsulated within ELP-HA hydrogels with varying HA concentration. Increasing HA concentration led to a dose-dependent increase in cartilage-marker gene expression and enhanced sGAG deposition while minimizing undesirable fibrocartilage phenotype. The use of adaptable protein hydrogels formed *via* dynamic covalent

[*]co-corresponding authors. [#]co-corresponding authors.

chemistry may be broadly applicable as 3D scaffolds with decoupled niche properties to guide other desirable cell fates and tissue repair.

Keywords

adaptable hydrogels; dynamic covalent chemistry; elastin-like protein (ELP); cartilage regeneration; hyaluronic acid

1. Introduction

Cartilage loss is the leading cause for osteoarthritis, which represents one of the most common joint degenerative diseases in the U.S., affecting more than 50% of the population above the age of 65. [1] Unfortunately, cartilage has very limited self-healing capacity due to its avascular nature and low cellularity. [2, 3] Current treatment relies on autologous cartilage graft, which is limited by donor site morbidity and insufficient donor supply. [4, 5] Tissue engineering offers an alternative strategy for cartilage repair by providing cells, signaling molecules, and an artificial environment in the form of a biomaterial-based scaffold that is conducive to tissue growth. [6, 7] Hydrogels are particularly attractive scaffolds for cartilage repair given their injectability as well as tunable mechanical and biochemical properties. [8-11] Hyaluronic acid (HA) is a linear polysaccharide found ubiquitously in articular cartilage and is involved in many cellular processes, including cellular signaling, differentiation, and matrix deposition. [12, 13] HA-based hydrogels have been employed as 3D niches for cartilage tissue engineering, with demonstrated efficacy for supporting cartilage matrix formation by chondrocytes and various stem cells. [14-16] In addition to the biochemical cues and polymer concentrations, [17-19] mechanical cues such as matrix stiffness have also been shown to play an important role in regulating cell fate and cartilage tissue formation [20, 21]. One limitation associated with previously reported HA hydrogels is that an increase in HA concentration is commonly coupled with an increase in mechanical stiffness, [19, 22, 23] posing a challenge in elucidating the biological functions of HA.

To decouple the matrix stiffness change from varying HA concentrations, here we report the synthesis and characterization of an adaptable elastin-like protein - hyaluronic acid (ELP-HA) hydrogel platform using dynamic covalent chemistry (DCC), a type of covalent bond that is able to form and break reversibly under equilibrium control. [24] Previous literature has shown that compared with hydrogels fabricated from stable covalent chemistry, cells encapsulated in hydrogels crosslinked with DCC can locally modify and overcome physical restrictions in 3D to to spread, extend processes, and migrate while maintaining the long-term integrity of the matrix. [25-27] Here DCC crosslinking was used to form ELP-HA hydrogels through dynamic hydrazone bond *via* the reaction between hydrazine-modified ELP (ELP-HYD) and aldehyde-modified HA (HA-ALD). Hydrogel stiffness can be tuned by controlling the ratio of ALD/HYD and the concentration of ELP-HYD or HA-ALD. Genetically engineered elastin-like proteins (ELPs), inspired by the sequence of the native matrix protein elastin, have been shown to promote chondrogenesis. [28, 29] In addition, ELP-based hydrogels can be designed to enable independent control of matrix stiffness and

cell-adhesive ligand density to study cell-matrix interactions. [30, 31] Combining the advantages of protein-engineered materials and DCC, we aim to develop hydrogels with decoupled mechanical stiffness and physiologically relevant range of HA concentration.

To evaluate the effects of HA concentration on cell-based cartilage regeneration, neonatal bovine chondrocytes were encapsulated within these ELP-HA hydrogels with varying HA concentration and cultured in chondrocyte growth medium for up to three weeks. To confirm that hydrogel stiffness is decoupled from HA concentration, shear storage modulus was characterized by oscillatory rheology. Cell phenotype and neocartilage formation were analyzed by gene expression, cell proliferation, quantitative biochemical assays, and histology.

2. Materials and Methods

2.1. Materials

Unless otherwise noted, all chemicals and solvents were of analytical grade and used as provided by the manufacturers. Sodium periodate, hyaluronic acid (sodium salt, MW: 1500 -1800 kDa), tert-butyl carbazate (t-BC), tri-Boc hydrazinoacetic acid, HATU, 4-methylmorpholine, trifluoroacetic acid (TFA), anhydrous dimethylformamide (DMF), and dichloromethane (DCM) were purchased from Sigma-Aldrich (St. Louis, MO, USA). 2,4,6-trinitrobenzene sulfonic acid (TNBS) was purchased from Thermo Scientific Inc. (Odessa, TX, USA).

2.2. Elastin-like protein (ELP) expression and purification

The design and synthesis of a modular recombinant ELP was previously reported, containing cell-adhesive domains and lysine residues to act as amine-reactive crosslinking sites. [32] Full amino acid sequence is provided in Supporting Information (Table S1). ELP was expressed and purified using standard recombinant protein technology. Briefly, protein sequences were cloned into pET15b plasmids, expressed in *Escherichia coli* (strain BL21(DE3)), and induced with 1 mM isopropyl β-d-1-thiogalactopyranoside (IPTG) at an OD_{600} of 0.8 for ~6 h. The harvested cell pellets were suspended, lysed by three freeze–thaw cycles, and purified by iterative inverse temperature-cycling as previously reported. [33] Protein molecular weight and purity were confirmed by sodium dodecyl sulfate polyacrylamide gel electrophoresis (SDS-PAGE). Purified ELP was dialyzed three times (10,000 MWCO, 12 h, 4 °C, deionized water) to desalt. The ELP was then lyophilized and stored at 4 °C until use.

2.3. Synthesis of ELP-HYD

Hydrazine-modified ELP (ELP-HYD) was synthesized using a slightly modified procedure according to the previously reported method. [25] Tri-Boc hydrazinoacetic acid (0.149 g, 0.37 mmol, 2 equiv. per amine) was dissolved in anhydrous DMF and activated with HATU (0.145 g, 0.37 mmol, 2.0 equiv.) and 4-methylmorpholine (102.2 μL, 0.925 mmol, 4.5 equiv.). The reaction was stirred for 5 min, and then ELP (MW: 37840, 0.5 g, 0.185 mmol amine) was added, and the reaction was allowed to proceed overnight at room temperature. The product was precipitated in ice-cold diethyl ether, dried, and treated with a solution of

2.5% tri-isopropylsilane in 50:50 DCM:TFA for 4 hours to remove the Boc group. The resulting compound was precipitated in ether, dissolved in deionized water, dialyzed four times (10,000 MWCO, 4 12 h, 4 °C, deionized water), and lyophilized.

2.4. Quantification of ELP-HYD modification efficiency

To quantify the modification efficiency, samples before the removal of Boc groups were assessed by ^{1}H NMR spectroscopy on a Varian Inova 500 MHz NMR spectrometer using deuterated dimethyl sulfoxide as a solvent. The modification efficiency was determined by comparing the integration of methyl protons of the Boc group with the aromatic protons of tyrosine in Boc-protected ELP-HYD. Each ELP molecule has 14 amine groups for modification and 4 tyrosine groups. Using the intensity of the tyrosine peak as a reference, the number of methyl protons of t-Boc group per macromolecule of ELP was determined. The percent of modified amine groups was then calculated as $x = [(y/(3 \cdot 9))/z] \cdot 100\%$, where x is the percent modification, y is the number of methyl protons of t-Boc per molecule, 3 is the number of t-Boc groups per hydrazine modification, 9 is the number of methyl protons per t-Boc group, and z is the number of primary amines per macromolecule.

2.5. Synthesis and FTIR characterization of HA-ALD

Aldehyde-modified HA (HA-ALD) was synthesized using a slightly modified procedure according to a previously reported method. [9] HA (0.4 g) was dissolved in H_2O at a concentration of 4 mg/mL. An aqueous solution of sodium periodate (648 mg and 1080 mg for samples 1 and 2, respectively) was added dropwise, and the reaction was stirred overnight at room temperature in the dark. Ethylene glycol (500 μL) was then added to inactivate any unreacted periodate. The reaction was stirred for 1 h at room temperature. The product was dialyzed (3,500 MWCO) against deionized water for 2 days and lyophilized. An FTIR spectrometer (Vertex 70, Bruker Optics) was used to identify the functional groups and confirm the successful oxidization of HA. Air was used as a background control, and a single measurement consisted of 32 scans with a resolution of 4 cm^{-1}.

2.6. TNBS assay for quantification of HA oxidation

The degree of HA oxidation was quantified using a slightly modified procedure according to the previously described method. [34] HA-ALD (25 μL, 0.6 wt%) was mixed with tert-butyl carbazate (t-BC, 25 μL, 30 mM) in 1% aqueous trichloroacetic acid for 24 h at room temperature. TNBS reagent (0.5 ml of aqueous 2% TNBS in 0.1 M sodium bicarbonate buffer, pH 8.5) was added to the reaction mixtures and incubated for 2h at 37 °C. A volume of 50 μL of the final mixture was diluted with 0.5 N hydrochloric acid and transferred into a 96-well plate. In parallel, a standard calibration curve was prepared using aqueous t-BC solutions (5-15 mM). The amount of unreacted t-BC in the reaction mixture was determined from absorbance readings (λ = 340 nm, SpectraMax M2 microplate reader) and further used to calculate the aldehyde content. All measurements were in triplicate.

2.7. Formation of ELP-HA hydrogels

Lyophilized ELP-HYD and HA-ALD were solubilized in chilled phosphate buffered saline (PBS) (1×, pH 7.4) at a stock concentration of 3.6 wt % and 3 wt %, respectively. Air

bubbles were removed by centrifugation, and the final solutions were kept on ice until use. By mixing ELP-HYD and HA-ALD stock solutions at a volume ratio of 1:1 at room temperature, the crosslinked hybrid ELP-HA (1.8 wt%, 1.5 wt%) hydrogel was formed. Stock concentrations were adjusted to make gels with different formulations.

2.8. Hydrogel mechanical characterization

Mechanical testing was performed on a stress-controlled rheometer (ARG2, TA Instruments) using a 20-mm diameter cone-on-plate geometry. Samples were allowed to gel *in situ* on the rheometer, and a humidity chamber was secured in place to prevent dehydration. For gelation time characterization, time sweeps were performed at an oscillatory stress of 4.74 Pa at 25 °C. To characterize hydrogel stiffness, angular frequency sweeps were conducted from 0.1 to 10 Hz with constant 5% strain amplitude. Storage (G') and loss (G'') moduli at 1 Hz were selected from the frequency sweep. All measurements were in triplicate. Mechanical characterization for cell-laden hydrogels showed comparable storage (G') and loss (G'') moduli (Figure S1).

2.9. Compression modulus testing

Compression modulus testing was performed on the hydrogels at a 10 μm/s strain rate in unconfined compression using an 8-mm, plate-on-plate geometry. Engineering strain was calculated as the change in the gap distance divided by the original gap distance. The compression modulus was determined by the initial slope of the normal stress–strain curve.

2.10. Chondrocyte isolation and culture

Hyaline articular cartilage was dissected from the femoropatellar groove of both stifle joints from a 3-day old calf (Research 87). Neonatal chondrocytes were isolated by digesting sliced cartilage thin pieces in high glucose DMEM supplemented with 1 mg/mL type II and type IV collagenases (Worthington Biochemical), 100 U/mL penicillin, and 0.1 mg/mL streptomycin (Gibco, Invitrogen) overnight at 37 °C in 5% CO_2. The digested suspension was then filtered through a 70-μm cell strainer and washed three times before centrifuging at 460 g for 15 min. Chondrocytes after encapsulation within ELP-HA hydrogels were continuously cultured in chondrocyte growth medium, which includes high-glucose DMEM (Gibco) containing 10% fetal bovine serum (Gibco), 100 U/mL penicillin, 0.1 mg/mL streptomycin, 50 μg/mL ascorbate-2-phosphate (A2P) (Sigma-Aldrich), 40 μg/mL proline (Sigma-Aldrich), 100 μg/mL non-essential amino acid (NEAA) (Gibco), and 100 μg/mL HEPES buffer (Sigma-Aldrich). Medium was changed every other day for 3 weeks of culture period.

2.11. In vitro cell encapsulation and cell viability assay

For cell encapsulation, cells were first mixed in ELP-HYD solution at a concentration of 30 M/mL. This cell suspension was then mixed with HA-ALD solution at a volume ratio of 1:1 to reach a final cell concentration of 15 M/mL. Cell viability was determined using Live/Dead cytotoxicity kit (Invitrogen) on day 0. To visualize the cell distribution within the hydrogel, hydrogels were immersed in Live/Dead reagent solution for 20 minutes and imaged using a Zeiss fluorescence microscope. For 3D projection, images were collected

using a Leica confocal microscope by creating z-stacks of around 250-μm depth with 3.9-μm intervals between slices and then processed into a 3D projection (Figure 1).

2.12. Gene expression RT-PCR

Total RNA from all three groups of hydrogels (ELP-1.5% HA, ELP-3% HA, and ELP-5% HA) were extracted from chondrocytes (n = 3 hydrogels/group) after 7 days of growth culture. The relative expression levels of the genes of interest (Sox9, Aggrecan, Type I and II Collagen, and matrix metallopeptidase 13 (MMP13)) were determined using the comparative C_T method (Qiagen), in which target gene expression was first normalized to that of the housekeeping gene encoding glyceraldehyde-3-phosphate dehydrogenase (GAPDH), then normalized by gene expression measured in the control group (day 1 neonatal chondrocytes).

2.13. Biochemical assays (Picogreen, DMMB, and hydroxyproline)

After 3 weeks of culture, all three groups of cell-laden ELP-HA hydrogels (n=3) were digested using papain solution (Worthington Biochemical) at 60 °C for 16 hr. Using lambda phage DNA (10 μg/mL) as standard, DNA content was quantified and measured using the PicoGreen assay (Molecular Probes) subtracting the acellular control backgrounds. Sulfated-glycosaminoglycan (sGAG) was measured using the 1,9-dimethylmethylene blue (DMMB) dye-binding assay with shark chondroitin sulfate (Sigma) as standard (0.0884 mg/mL). Total collagen content was quantified using acid hydrolysis followed by p-dimethylaminobenzaldehyde and chloramine T (Sigma).

2.14. Histological analysis and immunofluorescence staining

To visualize the neocartilage extracellular matrix (ECM) production and distribution, immunofluorescence staining of collagen I, II, and X was performed after 21 days of culture. The cell-hydrogel samples were harvested and fixed in 4% paraformaldehyde (PFA) for 1 h at room temperature and then transferred to 30% sucrose solution (Sigma) overnight at 4 °C before snap freezing in optimal cutting temperature (O.C.T). Sections were incubated for 15 min at 37 °C for enzymatic antigen retrieval, then incubated with blocking buffer (2% goat serum in 3% BSA) for 1 hr before incubation with rabbit polyclonal antibody to collagen type I, II, and X (diluted at 1:100) (Abcam) overnight at 4 °C. Secondary antibody was diluted at 1:200 (Alexa Fluor 488 goat anti-rabbit) with Hoechst (2 μg/ml, for nuclei staining), and sections were incubated with secondary antibody for 1 h at room temperature. Samples were mounted with mounting medium (Vectashield), and images were taken with a Zeiss fluorescence microscope. For sGAG histological staining, sections were first washed in distilled water to remove O.C.T., and then stained for cell nuclei with hematoxylin solution for 15 sec before washing in distilled water. Then the sections were destained quickly in acid alcohol (2-3 dips) and washed again with distilled water. Fast green solution was used to stain the sections of cytoplasma for 1 min and rinsed quickly with 1% acetic acid solution within 10 sec. Samples were lastly stained in 0.1% safranin O solution for 5 min before dehydrating with ethanol and xylene and mounting for imaging.

2.15. Statistical analysis

Storage modulus is represented as mean ± standard deviation. Statistical difference for the same sample under different temperatures was analyzed by t-test. Statistical difference between samples was analyzed by one way ANOVA, two-way ANOVA and Bonferoni's post test. For all statistical tests, a threshold value of $\alpha = 0.05$ was chosen, and a p-value at or below 0.05 indicated significance.

3. Results and discussion

3.1. Synthesis of ELP-HYD and HA-ALD

ELP-HYD was obtained by introducing hydrazine groups onto ELP through the reaction between tri-Boc hydrazinoacetic acid and primary amines on ELP, followed by removal of the Boc protecting groups (Figure. 1A). To determine the degree of hydrazine modification, Boc-protected ELP-HYD was analyzed using ^{1}H-NMR. By comparing the integration of methyl protons of the Boc group with the aromatic protons of tyrosine, the degree of hydrazine modification was determined to be ~ 80% (Fig. S2). HA-ALD was obtained by introducing aldehyde groups onto HA through reaction with sodium periodate (Fig. 1B). FTIR was performed to confirm successful aldehyde modification. Compared with unmodified HA, the spectrum of HA-ALD shows a newly formed peak at 1733 cm^{-1} (Fig. S3), which corresponds to the stretching vibration of the C=O bond created in the oxidation reaction. To control the stoichiometry of the DCC crosslinking, we varied the degree of aldehyde modification on HA to be 26% or 32%, as quantified using a TNBS assay.

3.2. Formation of ELP-HA hydrogels and rapid gelation kinetics

ELP-HA hydrogels were fabricated *via* simply mixing the two components ELP-HYD and HA-ALD (Fig. 1C). To measure the gelation time, *in situ* gelation was monitored using a rheometer at room temperature. A hybrid hydrogel rapidly formed upon mixing the two components, indicated by an increase in storage modulus (G') after 10 s, reaching a plateau of ~ 350 Pa within 1 min, compared to a much smaller loss modulus (G'') of ~ 15 Pa (Fig. 1D-E). The fast gelation is attributed to the rapid formation of dynamic covalent hydrazone linkages between the hydrazine and aldehyde groups at physiological conditions. [25, 35] Generally speaking, a fast gelation rate is desirable to prevent cell sedimentation and to enable homogeneous cell encapsulation within the matrix. [36] To evaluate if the gelation rate is fast enough for 3D cell encapsulation, neonatal bovine chondrocytes were encapsulated within the ELP-HA hydrogel, followed by Live/Dead staining and confocal microscopy imaging. 3D reconstruction of images for the cell-gel construct showed that cells were greater than 95% viable (Fig. S4) and homogeneously distributed throughout the hydrogel owing to the rapid gelation kinetics (Fig. 1F).

3.3. Effects of varying polymer concentration and ALP/HYD ratio on hydrogel stiffness

The stiffness of ELP-HA hydrogels are observed to largely depend on ELP concentration and the stoichiometric ratio of reactive groups in the dynamic covalent reaction. While maintaining a constant HA-ALD concentration, decreasing ELP-HYD resulted in a lower shear storage modulus, G' (Fig. 2A-B). In addition, decreasing the ELP-HYD concentration

resulted in less thermal-induced stiffening when the temperature was increased from 25 to 37 °C (Fig. 2A). This stiffening effect is caused by ELP thermal aggregation that occurs above the lower critical solution temperature (LCST). [37] Previous work from our group has demonstrated that adding hydrophilic compounds such as polyethylene glycol into ELP hydrogels can significantly decrease ELP aggregation. [31] Similarly, here we observed that increasing the concentration of the hydrophilic HA-ALD compound from 1 wt% (Fig. 2A) to 4 wt% (Fig. 2B), also resulted in less thermal-induced stiffening.

Of note, hydrogels fabricated with 4 wt% ELP-HYD and 4 wt% HA-ALD (Fig. 2B) have much lower G' at 25 °C compared to gels with the same ELP concentration and only 1 wt% HA (Fig. 2A-B). This atypical observation of lower gel stiffness at a higher polymer concentration is caused by the higher stoichiometric ratio of aldehyde to hydrazine groups (ALD/HYD) in the dynamic covalent reaction. Generally in hydrogel formulation, a stoichiometry close to 1:1 will minimize dangling chains and loops and will result in more perfect network connectivity. In contrast, an increased stoichiometric imbalance will cause more network imperfections that have a direct negative impact on the gel mechanical properties. [38] Comparing the stiffness between the gel with 2 wt% ELP-HYD and 4 wt% HA-ALD and the gel with 2 wt% ELP-HYD and 2 wt% HA-ALD, we find that the G' are nearly identical. Thus, the effect of increased polymer weight percentage is off-set by the increased stoichiometric imbalance for these two formulations. These data suggest that it should be possible to formulate a series of gels with decoupled HA concentration and initial stiffness through modification of the crosslinking stoichiometry.

Therefore, we further evaluated the effect of varying HA-HYD concentration on hydrogel stiffness while keeping ELP concentration at 2 wt%. In general, higher polymer concentrations led to increasing stiffness, although the stiffness was much less sensitive to HA concentration compared to ELP concentration (Fig. 2C). This is attributed to the fact that increasing HA concentration also results in a larger imbalance of the stoichiometric ratio and hence more network imperfections, which compensates for the overall increase in polymer weight percentage.

Based on these observations, we hypothesized that by strategically choosing an ELP concentration and tuning the stoichiometric ratio of aldehyde groups to hydrazine groups, it would be possible to fabricate a series of hydrogels with the same ELP concentration and similar initial stiffness, but variable HA concentration. First, we selected a relatively low ELP concentration of 1.8 wt% to minimize thermal stiffening effects. Next, we reduced the degree of HA oxidation to decrease the stoichiometric ratios, which partially offsets the stiffness loss resulting from ELP concentration decrease. Finally, for the formulation with the highest HA concentration, we increased the degree of HA oxidation to counter-balance the potential stiffness increase caused by higher polymer concentrations. It was confirmed that ELP-HA hydrogels fabricated with 1.8 wt% ELP and 1.5, 3, or 5 wt% HA had similar initial storage moduli of ~ 350 Pa and loss moduli less than 20 Pa (Fig. 2D, Fig. S5), and these materials were used for further cellular studies.

3.4. HA enabled chondrocytes to retain articular cartilage phenotype in a dose-dependent manner in 3D

To evaluate the effects of different HA concentrations on the phenotype of chondrocytes in 3D, we first quantified gene expression of cartilage markers including aggrecan (Agg), SRY (sex determining region Y)-box 9 (SOX9), and type II collagen (COL2). Increasing HA led to a dose-dependent increase in gene expression of all tested cartilage markers by chondrocytes, suggesting a positive role of HA in stimulating cartilage-forming capacity of chondrocytes (Fig. 3A-C). For articular cartilage tissue engineering, it is important to enhance the desirable hyaline cartilage phenotype while minimizing the undesirable fibrocartilage or hypertrophic phenotypes, which can be characterized by type I and type X collagens. [39, 40] Our data shows that chondrocytes encapsulated in all three groups exhibit low type X collagen expressions (Fig. 3D). Cells encapsulated in low HA concentration hydrogels exhibit up to a 100-fold upregulation of type I collagen (Fig. 3E) while increasing HA concentration to 5% downregulated the undesirable type I collagen expression. In addition to cartilage markers, we further examined the effects of HA concentration on matrix metallopeptidase-13 (MMP-13) gene expression, which is a marker for cartilage remodeling. [41, 42] Gene expression results show that decreasing HA concentration led to a dose-dependent upregulation of MMP-13 activity (Fig. 3F), suggesting that chondrocytes encapsulated within the low HA group induce a more extensive level of matrix degradation and remodeling. In addition to biochemical cues, hydrogel stiffness can also modulate cartilage formation and chondrocyte phenotype in 3D culture. [39] Previous study has shown that chondrocytes cultured within some soft hydrogels (500 Pa) cannot maintain their phenotype and lose cartilage-specific marker expression over time. [43] Interestingly, our hydrogel is within a comparable stiffness range (~350 Pa), yet it supports chondrocyte phenotype retention, suggesting HA may rescue the ability of chondrocytes to retain phenotype in soft hydrogels. This phenotype maintenance in soft gels may also be partially attributed to the selection of dynamic covalent crosslinks in the hydrogel design, which can be broken and reformed dynamically by the cells during matrix remodeling and ECM deposition.

3.5. HA modulates chondrocyte proliferation and matrix deposition in 3D

We next asked if varying HA concentration could also affect chondrocyte proliferation and new extracellular matrix deposition. To answer this question, we quantified DNA, cartilage-specific matrix sGAG, and total collagen from the three ELP-HA gels at day 21. DNA content data show that hydrogels containing low HA (1.5-3%) supported more robust chondrocyte proliferation in 3D, up to 13 fold compared to day 1 (Fig. 4A). Increasing HA concentration to 5% reduced cell proliferation to 5 fold (Fig. 4A). The trend of accumulated sGAG was opposite to that of cell proliferation, but is consistent with the trend of cartilage marker expression (Fig. 3A-C), with higher HA inducing more sGAG deposition (Fig. 4B). Different from the trends observed for either DNA or sGAG, total collagen content showed the highest production in the gel with intermediate HA concentration (Fig. 4C). It is important to note that the total collagen assay includes all types of collagen (e.g. type I collagen, type II collagen, and type X collagen, etc.), and reflects accumulated matrix production over time by all cells within the gel. As such, the trend of biochemical content may differ from gene expression, which reflects a snapshot of cell phenotype at a given time

point. It has been reported that an increase in matrix forming capacity is often accompanied by decreased cell proliferation. [44, 45] Our observation is consistent with these reports, as the highest HA concentration gel resulted in increased sGAG deposition (Fig. 4B) and decreased cell proliferation (Fig. 4A).

3.6. HA increased sGAG deposition while minimizing fibrocartilage phenotype

To gain insight into the effect of HA concentration on spatial organization of neo-cartilage formation over time, we performed Safranin-O staining of sGAG and immunostaining of type II collagen, key markers for articular cartilage. Increasing HA concentration substantially enhanced the intensity of sGAG staining (Fig. 5, Fig. S6), while the low (1.5%) HA group exhibited more diffusive sGAG deposition. We also performed staining for type II collagen, which was observed to form nodules comprising multiple cells, with each nodule on the order of 50-200 μm in diameter. Comparable total amount of type II collagen deposition was observed across all groups. In hydrogels containing lowest HA (1.5%), type II collagen nodules appeared to be smaller and more diffuse, whereas increasing HA concentration correlated with formation of larger type II collagen nodules as seen in both the 3% and 5% HA groups. In addition, we also observed a significant increase in the compressive modulus over three weeks of culture, which indicates enhanced mechanical functionality of the engineered cartilage construct (Fig. S7). Immunostaining of type I collagen, an undesirable fibrocartilage phenotype, decreased as HA concentration increased (Fig. 6), suggesting HA reduces fibrocartilage phenotype in a dose-dependent manner in our hydrogel platform. Furthermore, a minimal amount of type X collagen, a hypertrophy marker, was detected across all groups at day 21 (Fig. 6). Together, the 5% HA gel was the leading scaffold for promoting articular cartilage phenotype, with the highest gene expression of cartilage-specific markers (Fig. 3), more intense sGAG deposition (Fig. 5), and minimal type I collagen (Fig. 6).

Consistent with our observations, previous work has shown that the addition of HA within a biomaterial can improve chondrocyte proliferation and matrix production significantly. [46] Clinically, HA has been shown to improve joint lubrication and significantly improve chondrocyte proliferation and matrix deposition in a dose-dependent manner. [47] However, other reports have also shown some contradictory results suggesting that HA can interfere with the delivery of insulin-like growth factor-1 (IGF-1) signaling molecule to chondrocytes, thus affecting the chondrocyte phenotype to be more fibroblastic-like (i.e. deposit type I collagen). [48] These inconsistencies in the reported effects of HA on chondrocyte phenotype may be due to the lack of control over mechanical properties when making changes in HA concentration. In our platform, the mechanical stiffness of all HA-hydrogels was kept constant so that the biochemical effect of HA could be investigated without matrix stiffness as a confounding factor. The differential effects of various HA concentrations on cartilage tissue formation highlighted the importance of using decoupled mechanical and biochemical 3D scaffolds to probe optimal cell-matrix interactions in a controlled manner.

4. Conclusion

In sum, here we report an ELP-HA hydrogel platform for cartilage tissue engineering that allows varying HA concentration across a physiologically relevant range without changing matrix stiffness. Our results showed that increasing HA concentration led to a dose-dependent increase in cartilage-marker gene expression, enhanced sGAG deposition, and minimized undesirable fibrocartilage phenotype. Finally, the concept of decoupling the mechanical stiffness from biochemical properties in 3D scaffolds through the use of careful tuning of crosslinker stoichiometry may be broadly applicable to studying other cell types and their microenvironment cues in order to facilitate optimal scaffold design for tissue repair.

Supplementary Material

Refer to Web version on PubMed Central for supplementary material.

Acknowledgments

The authors acknowledge funding provided by NIH R01DE024772 (F.Y.), NSF CAREER award (CBET-1351289) (F.Y.), California Institute for Regenerative Medicine Tools and Technologies Award (RT3-07804) (F.Y.) and Stanford Chem-H Institute (F.Y.), National Institutes of Health (1 U19 AI116484-01 and 5 R21 EB018407-02), National Science Foundation (DMR 1508006), and California Institute for Regenerative Medicine (RT3-07948) (S.C.H.), Stanford Graduate Fellowship (D.Z.), Stanford Interdisciplinary Graduate Fellowship (D.Z.), and Kodak Fellowship (H.W.).

References

1. Hootman JM, Helmick CG. Projections of US prevalence of arthritis and associated activity limitations. Arthritis Rheum. 2006; 54(1):226–9. [PubMed: 16385518]
2. Sophia Fox AJ, Bedi A, Rodeo SA. The Basic Science of Articular Cartilage: Structure, Composition, and Function. Sports Health. 2009; 1(6):461–468. [PubMed: 23015907]
3. Tuli R, Li WJ, Tuan RS. Current state of cartilage tissue engineering. Arthritis Research & Therapy. 2003; 5(5):235–238. [PubMed: 12932283]
4. Raghunath J, et al. Biomaterials and scaffold design: key to tissue-engineering cartilage. Biotechnol Appl Biochem. 2007; 46(Pt 2):73–84. [PubMed: 17227284]
5. Buckwalter JA, Mankin HJ. Articular cartilage: degeneration and osteoarthritis, repair, regeneration, and transplantation. Instr Course Lect. 1998; 47:487–504. [PubMed: 9571450]
6. Nesic D, et al. Cartilage tissue engineering for degenerative joint disease. Advanced Drug Delivery Reviews. 2006; 58(2):300–322. [PubMed: 16574268]
7. Cancedda R, et al. Tissue engineering and cell therapy of cartilage and bone. Matrix Biol. 2003; 22(1):81–91. [PubMed: 12714045]
8. Kim IL, Mauck RL, Burdick JA. Hydrogel design for cartilage tissue engineering: a case study with hyaluronic acid. Biomaterials. 2011; 32(34):8771–82. [PubMed: 21903262]
9. Tan HP, et al. Injectable in situ forming biodegradable chitosan-hyaluronic acid based hydrogels for cartilage tissue engineering. Biomaterials. 2009; 30(13):2499–2506. [PubMed: 19167750]
10. Jin R, et al. Enzymatically-crosslinked injectable hydrogels based on biomimetic dextran-hyaluronic acid conjugates for cartilage tissue engineering. Biomaterials. 2010; 31(11):3103–3113. [PubMed: 20116847]
11. Toh WS, et al. Cartilage repair using hyaluronan hydrogel-encapsulated human embryonic stem cell-derived chondrogenic cells. Biomaterials. 2010; 31(27):6968–6980. [PubMed: 20619789]
12. Toole BP. Hyaluronan: From extracellular glue to pericellular cue. Nature Reviews Cancer. 2004; 4(7):528–539. [PubMed: 15229478]

13. Burdick JA, Prestwich GD. Hyaluronic Acid Hydrogels for Biomedical Applications. Advanced Materials. 2011; 23(12):H41–H56. [PubMed: 21394792]
14. Astachov L, et al. Hyaluronan and mesenchymal stem cells: from germ layer to cartilage and bone. Front Biosci (Landmark Ed). 2011; 16:261–76. [PubMed: 21196170]
15. Chung C, Burdick JA. Influence of Three-Dimensional Hyaluronic Acid Microenvironments on Mesenchymal Stem Cell Chondrogenesis. Tissue Engineering Part A. 2009; 15(2):243–254. [PubMed: 19193129]
16. Unterman SA, et al. Hyaluronic Acid-Binding Scaffold for Articular Cartilage Repair. Tissue Engineering Part A. 2012; 18(23-24):2497–2506. [PubMed: 22724901]
17. Nguyen LH, et al. Engineering articular cartilage with spatially-varying matrix composition and mechanical properties from a single stem cell population using a multi-layered hydrogel. Biomaterials. 2011; 32(29):6946–52. [PubMed: 21723599]
18. Moutos FT, Freed LE, Guilak F. A biomimetic three-dimensional woven composite scaffold for functional tissue engineering of cartilage. Nature Materials. 2007; 6(2):162–167. [PubMed: 17237789]
19. Chung C, et al. Influence of gel properties on neocartilage formation by auricular chondrocytes photoencapsulated in hyaluronic acid networks. Journal of Biomedical Materials Research Part A. 2006; 77A(3):518–525.
20. Martens PJ, Bryant SJ, Anseth KS. Tailoring the degradation of hydrogels formed from multivinyl poly(ethylene glycol) and poly(vinyl alcohol) macromers for cartilage tissue engineering. Biomacromolecules. 2003; 4(2):283–292. [PubMed: 12625723]
21. Park Y, et al. Bovine primary chondrocyte culture in synthetic matrix metalloproteinase-sensitive poly(ethylene glycol)-based hydrogels as a scaffold for cartilage repair. Tissue Engineering. 2004; 10(3-4):515–522. [PubMed: 15165468]
22. Bian LM, et al. The influence of hyaluronic acid hydrogel crosslinking density and macromolecular diffusivity on human MSC chondrogenesis and hypertrophy. Biomaterials. 2013; 34(2):413–421. [PubMed: 23084553]
23. Ananthanarayanan B, Kim Y, Kumar S. Elucidating the mechanobiology of malignant brain tumors using a brain matrix-mimetic hyaluronic acid hydrogel platform. Biomaterials. 2011; 32(31):7913–7923. [PubMed: 21820737]
24. Rowan SJ, et al. Dynamic covalent chemistry. Angew Chem Int Ed Engl. 2002; 41(6):898–952. [PubMed: 12491278]
25. McKinnon DD, et al. Measuring cellular forces using bis-aliphatic hydrazone crosslinked stress-relaxing hydrogels. Soft Matter. 2014; 10(46):9230–6. [PubMed: 25265090]
26. McKinnon DD, et al. Biophysically Defined and Cytocompatible Covalently Adaptable Networks as Viscoelastic 3D Cell Culture Systems. Advanced materials (Deerfield Beach, Fla). 2014; 26(6): 865–872.
27. Wang H, Heilshorn SC. Adaptable hydrogel networks with reversible linkages for tissue engineering. Adv Mater. 2015; 27(25):3717–36. [PubMed: 25989348]
28. Betre H, et al. Characterization of a genetically engineered elastin-like polypeptide for cartilaginous tissue repair. Biomacromolecules. 2002; 3(5):910–916. [PubMed: 12217035]
29. Betre H, et al. Chondrocytic differentiation of human adipose-derived adult stem cells in elastin-like polypeptide. Biomaterials. 2006; 27(1):91–99. [PubMed: 16023192]
30. Lampe KJ, Antaris AL, Heilshorn SC. Design of three-dimensional engineered protein hydrogels for tailored control of neurite growth. Acta Biomaterialia. 2013; 9(3):5590–5599. [PubMed: 23128159]
31. Wang H, et al. Hybrid elastin-like polypeptide-polyethylene glycol (ELP-PEG) hydrogels with improved transparency and independent control of matrix mechanics and cell ligand density. Biomacromolecules. 2014; 15(9):3421–8. [PubMed: 25111283]
32. Liu JC, Tirrell DA. Cell Response to RGD Density in Cross-Linked Artificial Extracellular Matrix Protein Films. Biomacromolecules. 2008; 9(11):2984–2988. [PubMed: 18826275]
33. Straley KS, Heilshorn SC. Independent tuning of multiple biomaterial properties using protein engineering. Soft Matter. 2009; 5(1):114–124.

34. Chen YC, et al. In situ forming hydrogels composed of oxidized high molecular weight hyaluronic acid and gelatin for nucleus pulposus regeneration. Acta Biomaterialia. 2013; 9(2):5181–5193. [PubMed: 23041783]
35. Kool ET, Park DH, Crisalli P. Fast Hydrazone Reactants: Electronic and Acid/Base Effects Strongly Influence Rate at Biological pH. Journal of the American Chemical Society. 2013; 135(47):17663–17666. [PubMed: 24224646]
36. Haines-Butterick L, et al. Controlling hydrogelation kinetics by peptide design for three-dimensional encapsulation and injectable delivery of cells. Proceedings of the National Academy of Sciences of the United States of America. 2007; 104(19):7791–7796. [PubMed: 17470802]
37. Nettles DL, Chilkoti A, Setton LA. Applications of elastin-like polypeptides in tissue engineering. Advanced Drug Delivery Reviews. 2010; 62(15):1479–1485. [PubMed: 20385185]
38. Zhou HX, et al. Counting primary loops in polymer gels. Proceedings of the National Academy of Sciences of the United States of America. 2012; 109(47):19119–19124. [PubMed: 23132947]
39. Adkisson, HDt, et al. The potential of human allogeneic juvenile chondrocytes for restoration of articular cartilage. Am J Sports Med. 2010; 38(7):1324–33. [PubMed: 20423988]
40. Adkisson HD, et al. In vitro generation of scaffold independent neocartilage. Clin Orthop Relat Res. 2001391 Suppl:S280–94. [PubMed: 11603712]
41. Goldring MB. Chondrogenesis, chondrocyte differentiation, and articular cartilage metabolism in health and osteoarthritis. Therapeutic Advances in Musculoskeletal Disease. 2012; 4(4):269–285. [PubMed: 22859926]
42. Borzi RM, et al. MMP-13 loss associated with impaired ECM remodelling disrupts chondrocyte differentiation by concerted effects on multiple regulatory factors. Arthritis and rheumatism. 2010; 62(8):2370–2381. [PubMed: 20506238]
43. Wang LS, et al. Modulation of chondrocyte functions and stiffness-dependent cartilage repair using an injectable enzymatically crosslinked hydrogel with tunable mechanical properties. Biomaterials. 2014; 35(7):2207–2217. [PubMed: 24333028]
44. Detamore MS, Athanasiou KA. Effects of growth factors on temporomandibular joint disc cells. Arch Oral Biol. 2004; 49(7):577–83. [PubMed: 15126139]
45. Ruijtenberg S, van den Heuvel S. Coordinating cell proliferation and differentiation: Antagonism between cell cycle regulators and cell type-specific gene expression. Cell Cycle. 2016; 15(2):196–212. [PubMed: 26825227]
46. Klangjorhor J, et al. Comparison of growth factor adsorbed scaffold and conventional scaffold with growth factor supplemented media for primary human articular chondrocyte 3D culture. BMC Biotechnology. 2014; 14(1):1–14. [PubMed: 24400649]
47. Akmal M, et al. The effects of hyaluronic acid on articular chondrocytes. Bone & Joint Journal. 2005; 87-B(8):1143–1149.
48. Yoon DM, et al. Addition of hyaluronic acid to alginate embedded chondrocytes interferes with insulin-like growth factor-1 signaling in vitro and in vivo. Tissue Eng Part A. 2009; 15(11):3449–59. [PubMed: 19426107]

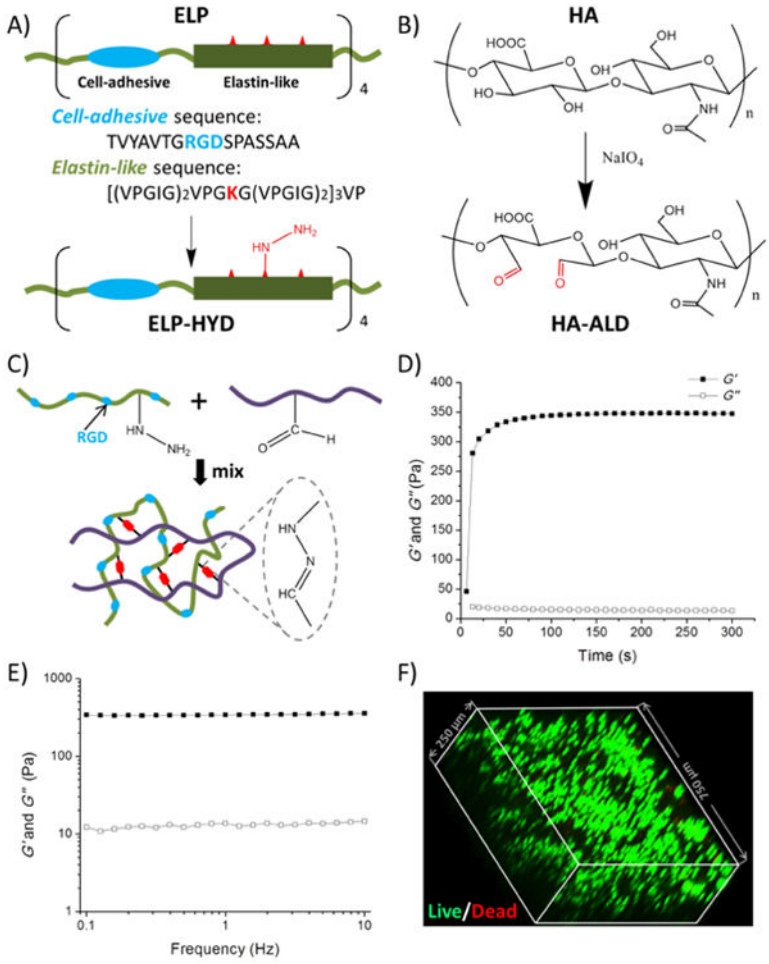

Figure 1.

Design and characterization of protein hydrogels for 3D cell encapsulation. (A) Elastin-like protein (ELP) was designed with four modular repeats of cell-adhesive (blue) and structural elastin-like (green) sequences. Lysine residues (red) were used to generate hydrazine-modified ELP (ELP-HYD). (B) Synthesis of aldehyde-modified hyaluronic acid (HA-ALD). (C) ELP-HA hydrogel is formed *via* reaction between hydrazines on ELP-HYD and aldehydes on HA-ALD to form dynamic covalent hydrazone linkages. (D & E) Rheological characterization of ELP-HA (1.8 wt%, 1.5 wt%) hydrogel during (D) an oscillatory time sweep at 25 °C to demonstrate onset of gelation and (E) an angular frequency sweep at 37 °C to demonstrate gel stability at physiological conditions. Storage moduli (G') are shown with filled symbols and loss moduli (G'') are shown with empty symbols. (F) Chondrocytes demonstrated round morphology and high viability after encapsulation in 3D ELP-HA hydrogels, as shown by confocal imaging of Live/Dead staining.

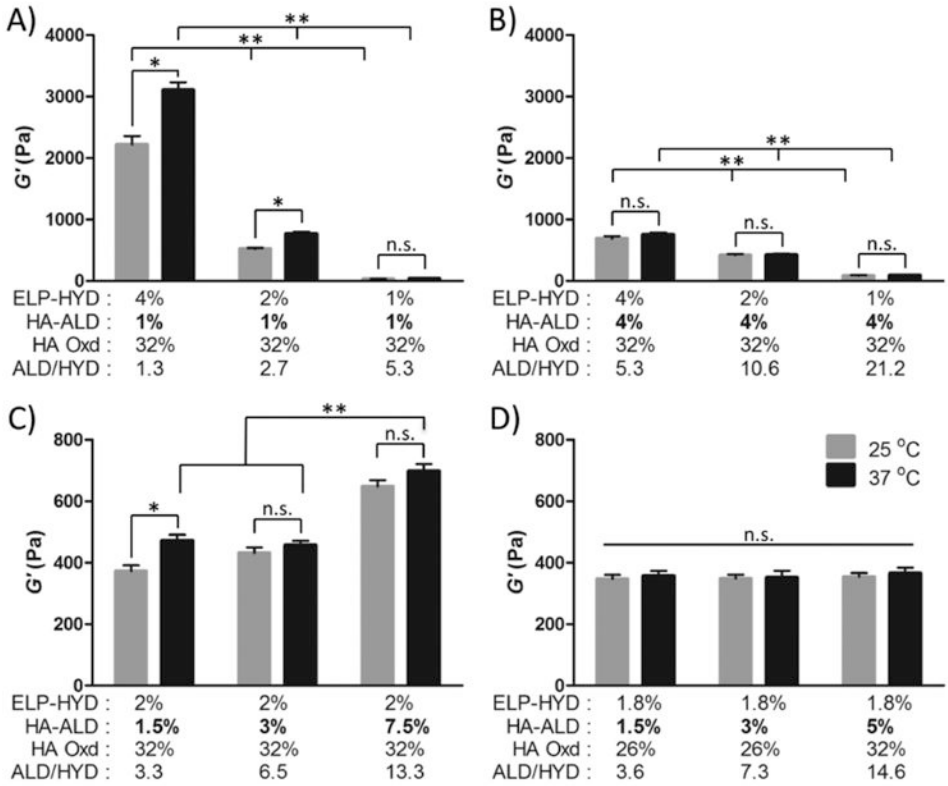

Figure 2.

Mechanical characterization of ELP-HA hydrogels at 25 °C (gray) and 37 °C (black). (A & B) Storage modulus response to variable ELP-HYD concentration of 4%, 2%, or 1% (w/v) and constant HA-ALD of (A) 1% (w/v) and (B) 4% (w/v). (C) Storage modulus response to variable HA-ALD concentration of 1.5%, 3%, or 7.5% (w/v) and constant ELP-HYD of 2% (w/v). (D) Storage moduli of final ELP-HA hydrogel formulations used for further cell studies. ELP-HYD concentration was fixed at 1.8% (w/v) while varying HA-ALD concentration (1.5%, 3%, 5%) (w/v). (* $p < 0.05$, t-test; ** $p < 0.01$, two way ANOVA and Bonferoni's post test)

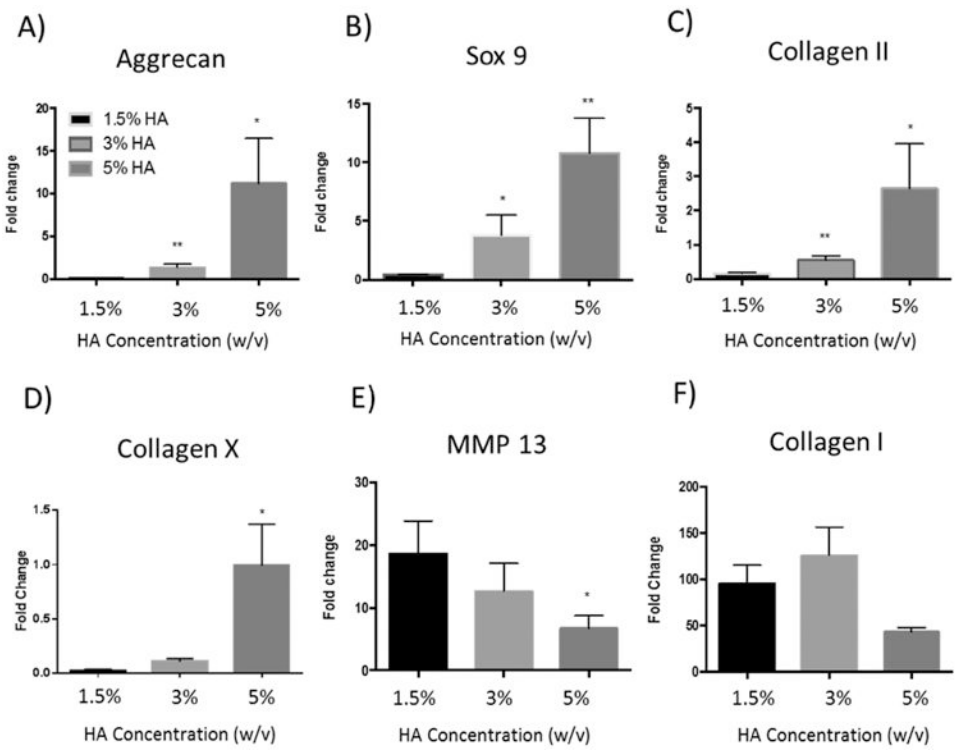

Figure 3.

Quantitative gene expression of cartilage markers by chondrocytes in three ELP-HA hydrogel compositions with varied HA concentrations after 7 days of culture in chondrocyte growth medium. HA concentrations were varied from 1.5% to 5% while keeping hydrogel stiffness constant (~350 Pa). (A) Aggrecan, (B) Sox 9, (C) type II Collagen, (D) type X Collagen, (E) matrix metallopeptidase (MMP13), and (F) type I collagen. Data are presented as average +/- standard deviation (n=3 per group). *p <0.1, **p<0.005 compared to ELP-1.5%HA group.

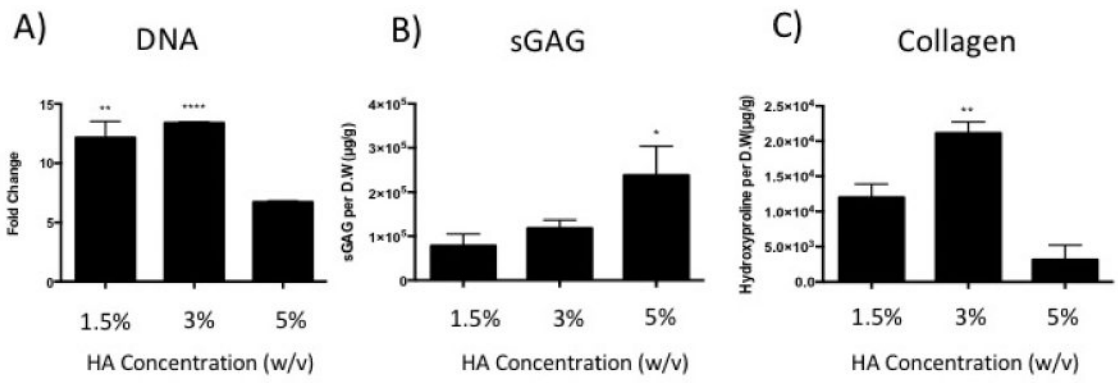

Figure 4.

Effects of varying HA concentration in 3D ELP-HA hydrogels on chondrocyte proliferation and cartilage matrix production. Quantification of (A) DNA content, (B) sulfated-glycosaminoglycan (sGAG) content, and (C) total collagen content. Data are presented as mean +/- standard deviation (n = 3 per group). **p<0.005; ****p <0.0001 compared with ELP-5% HA group in A) *p<0.05; **p<0.005 compared with ELP-1.5% HA group in B) and C).

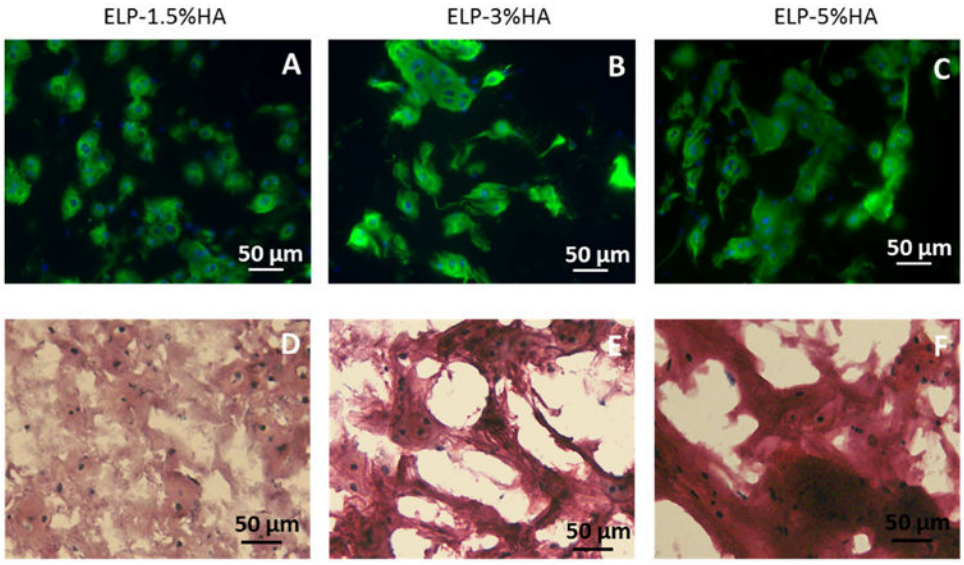

Figure 5.

The morphology of newly formed cartilage nodules (type II collagen and sGAG) by chondrocytes in ELP-HA hydrogels after 21 days of culture. (A-C) Immunostaining of type II collagen shows overall comparable amount of collagen II across the three groups, while the nodule size increases as HA increases; (D-F) Safranin O staining shows increasing HA concentration led to increased sulfated-glycosaminoglycan (sGAG) deposition. Scale bars: 50 μm.

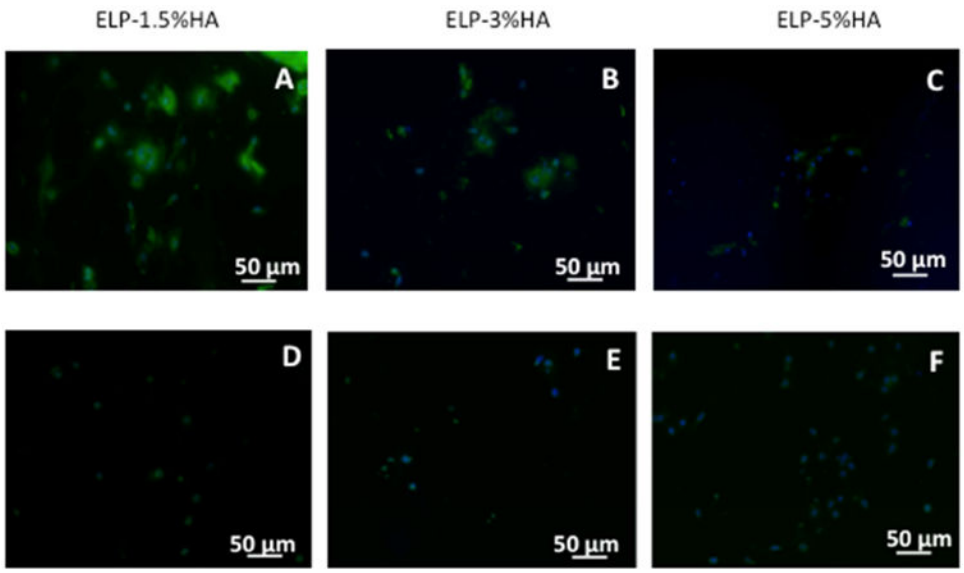

Figure 6.

Effects of varying HA concentration in ELP-HA hydrogels on fibrocartilage marker collagen I (A-C) and hypertrophy marker collagen X (D-F). Increasing HA concentration led to decreased type I collagen deposition. Minimal type X was detected in all groups. Scale bars: 50 μm.